MODELING THE ISOTOPE SIGNATURE OF METHANE AND DISSOLVED INORGANIC CARBON TO UNRAVEL METHANOGENIC AND OTHER FERMENTATION PATHWAYS IN BOREAL LAKE SEDIMENTS

François Clayer[1,3*], Yves Gélinas[2,3], André Tessier[1] & Charles Gobeil[1,3]

[1]Institut National de la Recherche Scientifique, Centre Eau Terre Environnement (INRS-ETE), Québec (Qc) Canada
[2]Department of Chemistry and Biochemistry, Concordia University, Montréal (Qc) Canada
[3]Geotop, Montréal (Qc) Canada
[*]Corresponding author: francois.clayer@ete.inrs.ca

INTRODUCTION

"CH_2O" is often used in models to represent organic matter (OM)[1]. Natural compounds have disparate carbon oxidation state (COS) and their fermentation does not necessarily yield equimolar amounts of methane (CH_4) and dissolved inorganic carbon (DIC).

- "CH_2O" is based on the **Redfield ratio from marine plankton**[2]

However,
- Lakes bury more OM[3] and release more CH_4 than the ocean[4]
- Most OM in freshwater sediments is terrigenous[5]

Is "CH_2O" suitable for representing the fermenting OM in boreal lake sediments?

Table 1: Influence of the COS on fermentation products

Compounds	Formula	COS	CH_4/DIC production ratio during fermentation
Glycolic acid [6]	$C_2H_4O_3$	+1.00	0.6
Glucose [6] (or CH_2O)	$C_6H_{12}O_6$	0.00	1.00
C_{16}-fatty acid [1]	$C_{16}H_{32}O_2$	−1.75	2.56
C_{16}-fatty alcohol [1]	$C_{16}H_{34}O$	−2.00	3.00

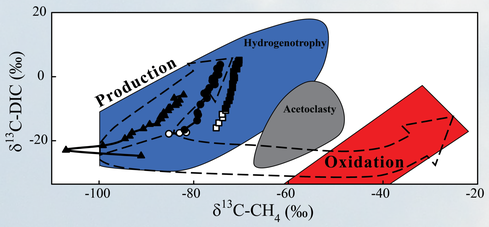

Figure 1: Combination plot of $\delta^{13}C$ of CH_4 and DIC[7]

Given that OM degradation reactions (Table 2), in particular methanogenesis and methanotrophy, influence the **carbon isotopic signature ($\delta^{13}C$)** of CH_4 and DIC (Fig. 1), we propose to simulate the $\delta^{13}C$ profiles and use it as a tool to:

1) Unravel sediment OM mineralization pathways

2) Test the robustness of the commonly-used model-molecule CH_2O

in **three boreal oligotrophic lakes** with **contrasted O_2 dynamics** (Fig. 2B).

MATERIALS & METHODS

CH_4, DIC and **oxidants** (O_2, NO_3^-, Mn(IV), Fe(III) and SO_4^{2-}) porewater concentrations were obtained by ***in situ*** **dialysis** (Fig. 2C) in
- L. Tantaré A — **oxic**
- L. Tantaré B — **seasonnally anoxic**
- L. Bédard — **anoxic**

The **$\delta^{13}C$ of CH_4** and **DIC** was determined with a gas-chromatograph coupled to an isotope-ratio mass-spectrometer (GC-C-IRMS).

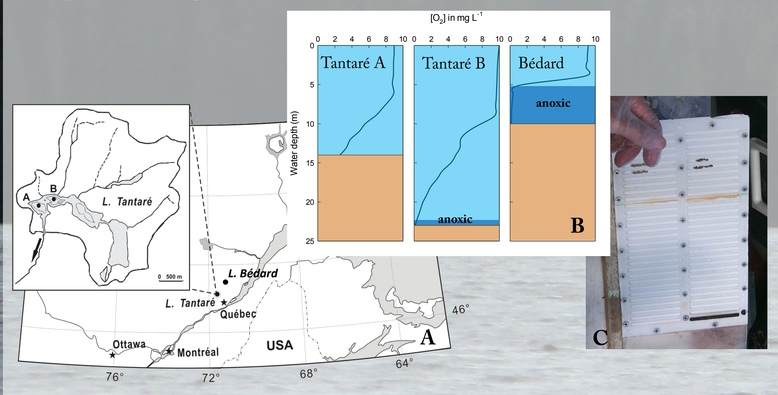

Figure 2: A - Location map, B - O_2 concentration profiles in each lake and C - Picture of a dialyser.

Inverse modeling of concentration profiles

Assuming **steady-state** conditions and neglecting advection and bioturbation, the diagenetic equation is:

$$\mathbf{1)}\quad \frac{\partial}{\partial x}\left(\varphi D_S \frac{\partial [sol.]}{\partial x}\right) + \varphi\alpha_B([sol.]_w - [sol.]) + R_{net}^{sol.} = 0$$

$[sol.]$ and $[sol.]_w$ are the solute concentrations in the porewater and the bottom water, respectively, x is the depth, φ is the porosity, D_S is the diffusivity, α_B is the bioirrigation coefficient, and $R_{net}^{sol.}$ the net reaction rate of the solute.

Eq. 1 is resolved via two numerical procedures, **PROFILE**[8] and **REC**[9], to:

Constrain the **depth-intervals** where solutes are produced or consumed (Table 3)

Obtain the R_{net} in each zone (thick lines in Fig. 3, Table 3)

Modeling the $\delta^{13}C$ profiles

Considering the isotopically heavy solute (^{13}C), **Eq. 1** becomes[10]:

$$\mathbf{2)}\quad \frac{\partial}{\partial x}\left(\varphi \frac{D_s}{f} \frac{\partial [^{13}C]}{\partial x}\right) + \varphi\alpha_B([^{13}C]_w - [^{13}C]) + R_{net}^{^{13}C} = 0$$

f is the molecular diffusivity ratio.

The term $R_{net}^{^{13}C}$ is the sum of the rates (R_i^*) of the isotopically heavy solute in reactions from Table 2.

R_i^* is given by[10]:

$$\mathbf{3)}\quad R_i^* = \frac{R_i [^{13}C]_i^{reactant}}{\alpha_i [C]_i^{reactant}}$$

R_i, α_i, $[..]_i^{reactant}$ are the rate, the fractionation factor and the reactant concentration, respectively, in the i^{th} reaction (Table 2). C denotes the total solute concentration.

Combining **Eq. 2** and **3** we obtain:

$$\mathbf{4)}\quad \frac{\partial}{\partial x}\left(\varphi \frac{D_s}{f} \frac{\partial [^{13}C]}{\partial x}\right) + \varphi\alpha_B([^{13}C]_w - [^{13}C]) + \sum_{i=1}^{5} \frac{R_i}{\alpha_i}\left(\frac{\delta^{13}C_i^{reactant}}{1000} + 1\right)\left(\frac{^{13}C}{^{12}C}\right)_{standard} = 0$$

$\delta^{13}C_i^{reactant}$ is the $\delta^{13}C$ of the reactant[11] in the i^{th} reaction

Eq. 4 is resolved via MATLAB® to obtain a **modeled $\delta^{13}C$ profile** (**lines** in Fig. 4).

RESULTS & DISCUSSION

Table 2: Reactions considered during sediment OM degradation

Reactions	Equation, reaction rate (R_i) and fractionation factor (α_i)		
1) OM fermentation	$C_xH_yO_z + (x+v-z)H_2O \rightarrow 1/2(x-v)CH_3COOH + vCO_2 + (y/2-z+2v)H_2$	R_1	α_1
2) Acetoclasty	$CH_3COOH \rightarrow CH_4 + CO_2$	R_2	α_2
3) Hydrogenotrophy	$CO_2 + 4H_2 \rightarrow CH_4 + 2H_2O$	R_3	α_3
4) Methanotrophy	$CH_4 + 2Oxidants \rightarrow CO_2 + 2Reducers$	R_4	α_4
5) OM oxidation	$CH_2O + Oxidant \rightarrow CO_2 + Reducer$	R_5	α_5

From **Table 2**, we can write:

$$R_{net}^{DIC} = R_1 + R_2 - R_3 + R_4 + R_5 \qquad R_{net}^{CH_4} = R_2 + R_3 - R_4$$

$$R_{net}^{oxidant} = -2R_4 - R_5$$

These equations and the values of $R_{net}^{sol.}$ in each zone (Table 3) are used to constrain all the possible R_i values. For example, CH_4 is produced in Zone 3 at about the same rate than DIC is consumed suggesting that hydrogenotrophy is the only reaction. Several scenarios for each lake are compared (Fig. 5A) and the best one is selected by fitting the simulated and measured $\delta^{13}C$ profiles (Fig. 4).

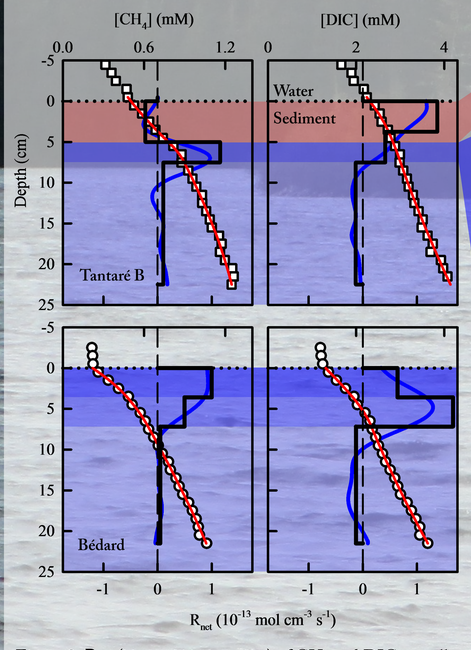

Figure 3: R_{net} (**blue and black profiles**) of CH_4 and DIC as well as their measured (**symbols**) and modeled (**red profile**) concentrations.

This modeling approach reveals that:

- **Methanogenesis is ~100 % hydrogenotrophic in the three lakes**
- **Hydrogenotrophy co-occurs with CH_4 and OM oxidations**
- **The fermentation of OM yields 1.5–3 times more CH_4 than DIC suggesting that the organic substrate is more reduced than CH_2O**
- **Considering that H_2 comes from reaction 1 only, the COS† of the fermenting OM is:**

Tantaré A: ≤ −0.76 **Tantaré B: −1.87** **Bédard: ≤ −0.85**

†Fell free to ask the presenter for calculation details

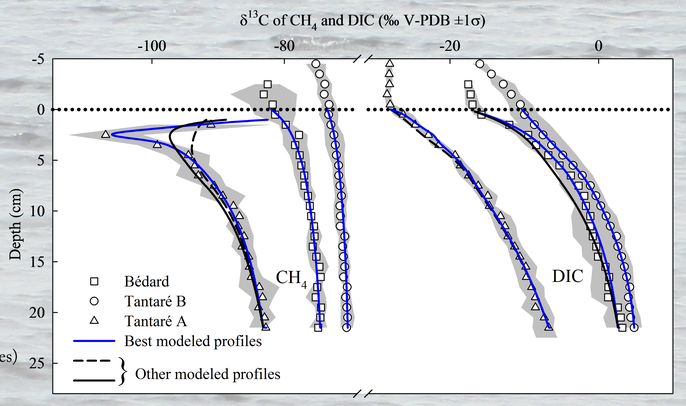

Figure 4: Measured (symbols) and modeled (blue and black profiles) $\delta^{13}C$ of CH_4 and DIC.

Table 3: Net reaction rates for each solute obtained with PROFILE

Lake	Zones	R_{net}^{DIC}	$R_{net}^{CH_4}$	$R_{net}^{oxidant}$
		(fmol cm^{-3} s^{-1})		
Tantaré A	1	223	−7	−335
	2	113	39	−103
	3	−2	1	
Tantaré B	1	114	−23	−25
	2	42	116	
	3	−13	11	
Bédard	1	65	100	−6.5
	2	167	50	−4.5
	3	−13	5	

The accurate fitting between the measured and modeled $\delta^{13}C$ profiles also allows **constraining the α_i** of OM mineralization reactions (Fig. 5B).

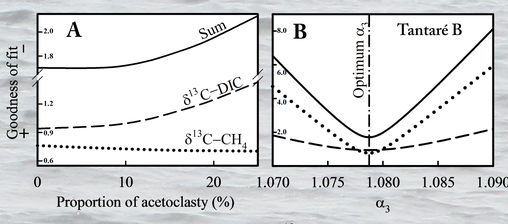

Figure 5: Goodness of fit for the $\delta^{13}C$ profiles in Tantaré B as a function of the percentage of acetoclasty (A) and the value of α_3 (B). The goodness of fit is estimated with the norm of residuals (small numbers along the y axis), i.e., the sum of the absolute differences between the measured datapoints and simulated profiles. Feel free to ask the presenter for graphs from other lakes.

CONCLUSION

1) Considering that, in these oligotrophic lakes:
- **methanogenesis is 100% hydrogenotrophic**
- **the COS of OM is negative (< −0.8)**

the OM formulation in boreal lakes should be revised.

2) Why does hydrogenotrophy become important with sediment depth[12] or as primary production drops[13]?

When labile OM is depleted, hydrogenotrophy is predominant[14] and **possibly fueled by reduced OM.**

ACKNOWLEDGEMENTS

Fonds de recherche Nature et technologies Québec

CRSNG NSERC

Permission to work in the Tantaré Ecological Reserve from the *Ministère [...] de l'Environnement* is acknowledged. We also thank: L. Rancourt, P. Girard, J.-F. Dutil, A. Royer-Lavallée, A. Laberge, A. Moritz, A. Barber and J.-F. Hélie (UQÀM; $\delta^{13}C$ standard).

REFERENCES

[1]**Arning** E. T., van Berk W. & Schulz H.-M. (**2016**) Marine Chemistry 178, 8–21.
[2]**Hedges** J.I., Baldock J.A., Gélinas Y., et al. (**2002**) Marine Chemistry 78, 47–63.
[3]**Tranvik** L.J., Downing J.A., Cotner J.B., et al. (**2009**) Limnology & Oceanography 54, 2298–2314.
[4]**Bastviken** D., Cole J., Pace M. & Tranvik L. (**2004**) Global Biogeochemical Cycles 18, GB4009.
[5]**Hedges** J.I. & Oades J.M. (**1997**) Organic Geochemistry 27, 319–361.
[6]**Larowe** D. E. & Van Cappellen P. (**2011**) Geochimica et Cosmochimica Acta 75, 2030–2042.
[7]**Whiticar** M. J. (**1999**) Chemical Geology 161, 291–314.
[8]**Berg** P., Risgaard-Petersen N. & Rysgaard S. (**1998**) Limnology and Oceanography 43, 1500–1510.
[9]**Lettmann** K.A., Riedinger N., Ramlau R., Knab N., et al., (**2012**) Estuarine, Coastal and Shelf Science 100, 26–37.
[10]**Alperin** M. J., Reeburgh W. S. & Whiticar M. J. (**1988**) Global Biogeochemical Cycles 2(3), 279–288.
[11]**Conrad** R., Claus P., Chidthaisong A., et al. (**2014**) Organic Geochemistry 73, 1–7.
[12]**Conrad** R., Claus P. & Casper P. (**2009**) Limnology & Oceanography 55, 1932–1942.
[13]**Galand** P.E., Yrjälä K. & Conrad R (**2010**) Biogeosciences 7, 3893–3900.
[14]**Hornibrook** E.R.C., Longstaffe F.J. & Fyfe W.S. (**2000**) Geochimica et Cosmochimica Acta 61, 745–753.